Influence of the molar masses on compatibilization mechanism induced by two block copolymers in PMMA/PS blends

Julie Genoyer,[1,2] Jérémie Soulestin,[1] and Nicole R. Demarquette[2,a)]

[1]*IMT Lille Douai, Department of Polymers and Composites Technology and Mechanical Engineering, 59500 Douai, France*

[2]*École de Technologie Supérieure, Department of Mechanical Engineering, Montreal, Quebec H3C 1K3, Canada*

(Received 12 October 2017; final revision received 20 March 2018; published 9 April 2018)

Abstract

The compatibilization mechanism of poly(methylmethacrylate) (PMMA)/polystyrene (PS) blends induced by PMMA-*b*-PS block copolymers of different molar masses (30 and 104 kg/mol) was studied. The blend morphologies with and without copolymers were observed by scanning electron microscopy. The rheological behavior was studied performing small amplitude oscillatory shear experiments. The experimental results were compared to Palierne's model predictions. Shear induced coalescence tests were also conducted. Contrary to what was expected, adding block copolymers did not result in a refinement of the droplet size. However, it induced Marangoni stresses, a decrease in interfacial tension and an inhibition of coalescence of the dispersed phase. During coalescence tests, a decrease in the relaxation time due to Marangoni stresses with time was revealed. This interesting behavior contradicts previous works on the subject, and is believed to be due to a migration of block copolymers to the interface during the tests rather than droplets' coalescence. As such, the morphology was explained by the fact that block copolymers are not entirely at the interface initially. Also, the block copolymer with a higher molecular mass was shown more efficient at inhibiting coalescence, indicating that the compatibilization mechanism is a combination of Marangoni stresses and steric hindrance. © *2018 The Society of Rheology*. https://doi.org/10.1122/1.5009047

I. INTRODUCTION

The control of the morphology of immiscible polymer blends is a common issue in polymer processing. When polymer blends are subjected to flow, their morphology is influenced by breakup and coalescence phenomena. Taylor [1] suggested that at low stress in a steady uniform shear flow, the deformation degree of a droplet is a function of

- the capillary number Ca

$$Ca = \frac{F_{\text{viscous}}}{F_{\text{interfacial}}} = \frac{\eta_m \dot{\gamma} R_v}{\alpha}, \tag{1}$$

- the viscosity ratio p

$$p = \frac{\eta_d}{\eta_m}, \tag{2}$$

where η_m and η_d are the viscosities of the matrix and the droplets, respectively, $\dot{\gamma}$ is the shear rate, R_v is the radius of the droplets, and α is the interfacial tension.

Applying a flow can lead to droplet breakup when the interfacial tension forces cannot balance the viscous forces. That is what happens above a critical value of the capillary number Ca_c. Below this value the coalescence will be promoted. Grace [2] provided data about this phenomenon by experimentally plotting Ca_c as a function of p for both simple shear and extensional flow (Fig. 1). The lowest Ca_c, in other words, the range where breakup is the easiest, is found for $0.1 \leq p \leq 1.0$. This is the range where most blends will be chosen as a fine morphology is wanted for good final properties; however, coalescence still often takes place during processing.

The addition of a so-called compatibilizer is a way to control the morphology over time [3,4]. Premade block copolymers (BCs) are generally used for this purpose, but at the industrial level, it is more common to create a compatibilizer during processing, thanks to an interfacial reaction [5]. For both methods, in the case of a droplet dispersion, the compatibilizers settle at the interface because of their dual chemistry. Their addition leads to a reduction of the dispersed phase size [6–8], an inhibition of the droplet's coalescence [9–13], a decrease in interfacial tension [7–9,14], and the presence of an additional relaxation phenomenon [14–22] besides an improvement of the blend properties.

Coalescence suppression is generally believed to be induced by two phenomena. The first one is based on the appearance of Marangoni stresses. When two droplets approach each other, the matrix flows out from the gap between the approaching droplets and when it happens the compatibilizer is dragged along. This results in a gradient in compatibilizer concentration on the droplet surface, so in an interfacial tension gradient. Because of that, Marangoni stresses appear to make the compatibilizer come back

a)Author to whom correspondence should be addressed; electronic mail: nicoler.demarquette@etsmtl.ca

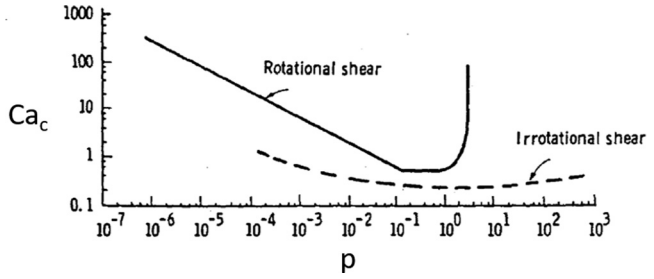

FIG. 1. Effect of the viscosity ratio on critical capillary number in rotational shear and irrotational shear fields [2].

homogeneously around the droplets and in doing so prevents coalescence. Those Marangoni stresses are the source of the additional relaxation phenomenon mentioned previously. They were evidenced by Jeon and Macosko [23] who showed gradients in BC concentration during flow by visualizing a fluorescent polystyrene (PS)-poly(methylmethacrylate) (PMMA) copolymer at the surface of a PMMA droplet in a PS matrix. The minimum coverage of BC necessary to completely suppress coalescence by considering Marangoni stresses can be estimated using the following equation[24]:

$$\sum_{\min} = \frac{5}{32}\frac{2R_v\eta_m\dot{\gamma}}{kT}. \tag{3}$$

The second mechanism, proposed by Sundararaj and Macosko [9], explains coalescence suppression by steric hindrance. When two droplets approach each other, the BC is squeezed in between them. It leads to repulsion between the droplets because a change in the conformation of the copolymer chain leads to a gain in entropy. This hypothesis is consistent with the observations of Van Hemelrijck *et al.* [17], and Lyu *et al.* [13] that showed that the length of the diblock in the matrix influences coalescence in such a manner that the longer the block, the more coalescence is suppressed. This theory assumes that the BC cannot move at the interface. By equating the Van der Waals force with the steric force, the minimum coverage of BC can be estimated by the following expression [13]:

$$\sum_c = \frac{20}{27\pi\langle r_0^2\rangle}, \tag{4}$$

where $\langle r_0^2\rangle$ is the square mean end-to-end distance of the chains of BCs. Originally, this steric hindrance theory was developed to explain suppression of static coalescence; thus, it is independent of shear rate.

These two phenomena could also be present at the same time, but this is rarely dealt with in the literature. On this subject, Fortelný [20] assessed that steric hindrance can act only if the Marangoni effect is negligible, suggesting that Marangoni stresses usually dominates. All these are valid if the BCs settle only at the interface; however, some researchers evidenced that micelles can be present in the blends, decreasing the efficiency of the compatibilizers [24]. The efficiency is then linked to the quantity of BC at the interface, thus to the surface coverage.

The rheological characterization of a blend in the linear regime can provide information on the morphology, interfacial tension between the polymers forming the blend and relaxation phenomena mentioned above. Indeed, small amplitude oscillatory shear (SAOS) experiments reveal an increase in elasticity at low frequencies, resulting in a shoulder on the storage modulus curve as a function of frequency. This increase is associated with the relaxation of the shape of the droplets (τ_F), which were previously deformed by the stress applied [25]. In the case of compatibilized blends, an additional relaxation time (τ_β) may be observed. Van Hemelrijck *et al.* [16] showed that τ_F depends mainly on the concentration of the dispersed phase, whereas τ_β strongly depends on the concentration of compatibilizer. Therefore, the latter relaxation time is believed to be due to the presence of copolymer at the interface, and especially to the presence of Marangoni stresses.

In order to evaluate clearly relaxation times, relaxation spectra can be recovered from classical small amplitude oscillatory shear measurements using Honerkamp and Weese method [26]. Those spectra allow a better visualization of the relaxation times originated from the relaxation of the droplet shape and Marangoni stresses. In the present work, these relaxation times will be called droplet's shape relaxation and Marangoni's relaxation.

Several models have been developed to link the rheological behavior of polymer blends to their morphology. One such model is Palierne's model, which predicts the rheological behavior of a blend formed by two viscoelastic polymers [27]. The polymers should be viscous enough to render bulk forces such as gravitation and inertia negligible, and the emulsion should be monodispersed and diluted. This model is made to predict the behavior of blends in the linear viscoelastic regime, in other words at small and slow deformations. As such, the constitutive equations which relate stress to deformations are linear. This model predicts the relaxations happening in a blend.

The simplified version commonly used gives the following expression for the droplet's shape relaxation time [28]:

$$\tau_F = \frac{\left(\frac{R_v\eta_M}{4\alpha}\right)(19p+16)(2p+3-2\Phi(p-1))}{10(p+1)-2\Phi(5p+2)}, \tag{5}$$

where R_v is the average droplet radius, α the interfacial tension, and Φ the volume fraction of the dispersed phase.

The original Palierne model was modified by Jacobs *et al.* [15] [see Eqs. (6)–(9)] to take into account Marangoni's relaxation (τ_β), resulting in values for both the droplet shape and Marangoni stress relaxation times as follows:

$$\tau_F = \frac{\lambda_{12}}{2}\left(1-\left(1-\frac{4\lambda_{11}}{\lambda_{12}}\right)^{0.5}\right), \tag{6}$$

$$\tau_\beta = \frac{\lambda_{12}}{2}\left(1+\left(1-\frac{4\lambda_{11}}{\lambda_{12}}\right)^{0.5}\right). \tag{7}$$

With

$$\lambda_{11} = \frac{R_v \eta_m}{4\alpha} \frac{(19p+16)(2p+3-2\Phi(p-1))}{10(p+1)+\frac{\beta_{20}}{\alpha}(13p+12)-2\Phi\left((5p+2)+\frac{\beta_{20}}{2\alpha}(13p+8)\right)}, \tag{8}$$

$$\lambda_{12} = \frac{R_v \eta_m}{8\beta_{20}} \frac{10(p+1)+\frac{\beta_{20}}{\alpha}(13p+12)-2\Phi\left((5p+2)+\frac{\beta_{20}}{2\alpha}(13p+8)\right)}{(1-\Phi)}, \tag{9}$$

where β_{20} is the interfacial shear modulus, an interfacial parameter.

In the present work, PMMA/PS blends with the addition of PS-*b*-PMMA BCs of different molar masses were studied. PMMA/PS blends are often used as "model" blends for research as their rheological behavior is well known and not too much sensitive to side effects like degradation. The morphology and rheological behavior were assessed. The interfacial tension was calculated using Palierne's model. The compatibilization mechanism was studied using rheology: Marangoni stresses were evidenced using the relaxation spectra inferred from SAOS measurements, and shear induced coalescence tests were performed.

II. MATERIALS AND METHODS

A. Materials

In this study, PMMA from PLEXIGLAS, grade 6N, and PS from INEOS Styrenics, grade EMPERA 350N, were used. Two symmetric (ratio PMMA/PS 1:1) BCs with their molar mass being the only difference were added to the blends. The BCs were purchased from Sigma Aldrich. The characteristics of the materials are reported in Table I.

B. Blending

Blends of PMMA/PS in 90/10 weight concentrations were prepared. To these were added different concentrations of BC ranging from 0 to 1 wt. %. All the percentages in this paper are weight percentage.

The blends were prepared using a microtwin screw extruder HAAKE MiniLab II from Thermo Scientific. Components were blended at 200 °C and 50 rpm after PMMA was dried at 80 °C for at least 12 h. Blends were prepared in two steps: First, the BCs were mixed with the minor phase (PS) in direct extrusion mode, and then, PS + BC was mixed with PMMA for 7 min in cycle extrusion mode. The aim was to follow a process similar to another work [29]. In the case of the uncompatibilized PMMA/PS blend (without BC, called pure in the rest of the paper), the minor phase was processed twice in order to ensure it had the same thermal history as the others.

TABLE I. Properties of the polymers.

Polymer	M_n (g/mol)	M_w/M_n	Melt flow index (cm^3/10 min)	Viscosity (η_0) (Pa s) at 200 °C
PMMA	—	—	12 (230 °C/3.8 kg)	12 000
PS	—	—	1.5 (200 °C/5 g)	9 800
BC1	30 000	≤1.2		—
BC2	104 000	≤1.2		—

C. Characterizations

Samples for rheological and morphological analyses, discs with a 25 mm diameter and 1 mm thickness, were molded at 200 °C under 18 MPa for 10 min using a compression molding press.

The rheological characterization was performed using two stress-controlled rheometers: MCR 501 and MCR 302 from Anton Paar. All measurements were carried out under dry nitrogen atmosphere. A parallel-plate geometry was used with a gap size of 0.9 mm and plate diameter of 25 mm. Time sweep tests were performed in order to check the thermal stability of the samples and showed that the samples were stable at 200 °C for 2 h. Strain sweep tests were carried out for blends and pure polymers to define the linear viscoelasticity region. The strain was fixed at 4% in the linear region. Finally, dynamic frequency sweep tests were performed from 300 to 0.01 Hz for all blends and pure polymers at 200 °C and some at 180 °C. The zero-shear viscosity of the individual phases necessary for further analyses and calculation was determined using the curve of complex viscosity (Pa s) versus frequency (rad/s) from dynamic frequency sweep tests. Rheological experiments were shown to be reproducible within 5% for both rheometers.

Coalescence tests were conducted on the MCR 302 at 200 °C under nitrogen. As the blend already has a fine morphology, a preshearing was not considered necessary. The shear rate was chosen low enough to favor coalescence: Using $p = 0.82$, the experimental fit of Grace's curve by Tucker and Moldenaers [4] [Eq. (10)] gives a critical capillary number of 0.47. Equation (1) gives a critical shear rate of 0.12 s^{-1} [using η_m from Table I and $R_v = 0.323\ \mu$m, R_v of the pure blend measured by scanning electron microscopy (SEM)]. Thus, a shear rate of 0.05 s^{-1} was chosen to ensure coalescence conditions. The coalescence tests were designed as described in Fig. 2 with a succession of steady shear (shear induced coalescence) and frequency sweeps to probe the evolution of morphology as first described in the work of Vinckier *et al.* [30],

$$\log Ca_c = -0.506 - 0.0995\log p + 0.124(\log p)^2 - \frac{0.115}{\log p - \log 4.08}. \tag{10}$$

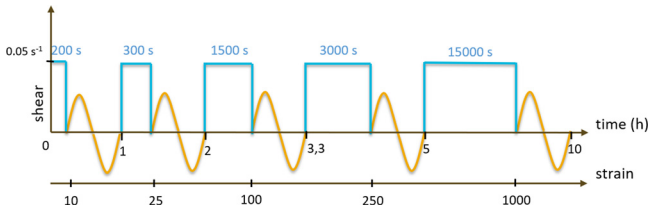

FIG. 2. Design of coalescence experiments.

Those tests last 10 h in total. The rheological behavior is then evaluated as a function of strain [(time length of steady shear) × (shear rate)]. Neat polymers were characterized rheologically. Table II shows the evolution of the zero shear viscosity and the resulting viscosity ratio during the tests. During coalescence tests, some thermal degradation occurs resulting in a decrease in PMMA and PS viscosity. These data were taken into account at each step of the test. BCs probably also degrade during coalescence tests. This degradation is considered to be taken into account by considering PMMA and PS decrease in viscosity as their degradation will be similar and also because the amount of BC is very low.

The morphology prior to coalescence was characterized by SEM using a HITACHI SU8230 FE-SEM. A JEOL JCM-600 plus was used for blends after coalescence. The samples were previously fractured at ambient temperature. For the use of JEOL JCM-600 plus, the samples were covered with gold. The morphology was quantified with ImageJ software considering at least 600 particles for each sample.

III. RESULTS AND DISCUSSION

A. Morphology

SEM observations were used to assess morphology. Small droplets were obtained, but contrary to what has been observed in many other studies, the addition of BC did not result in a decrease in the droplets average volume radius (see Figs. 3 and 4). For PMMA/PS systems, Yee *et al.* [8] showed a decrease in R_v with the addition of random BC.

An explanation could be that there are micelles in the blend which would limit the amount of BC at the interface, thus limiting the compatibilization mechanism. However, because of their dual chemistry, it is expected that at least part of the BC is at the interface. In this case, the interfacial tension should be decreased [4,16,17] and Marangoni stresses should appear [18,19].

TABLE II. Evolution of complex viscosities of PMMA and PS and of the resulting viscosity ratio p during coalescence tests at 200 °C.

Strain	0	10	25	100	250	1000
η_0 (PMMA)	11 900	11 800	11 500	11 100	10 700	9800
η_0 (PS)	9800	7100	6200	5900	5700	5200
p	0.82	0.60	0.54	0.53	0.53	0.53

B. Interfacial tension and Marangoni stresses

To verify if there are BCs at the interface, rheological experiments were conducted at 200 °C. Figures 5(a) and 5(b) show the storage moduli of the blends as a function of frequency. It can be seen that the presence of BCs induces an increase in G′ even at high frequencies. This could indicate the presence of BCs in one of the phases, however, this cannot be ensured here. As the concentration of dispersed phase and BC is very low, the shoulder that should be present on the storage modulus, in the case of BC at the interface [16], is not apparent. In order to better visualize the relaxation phenomena, the relaxation spectra of the blends were calculated using the SAOS data reported in Figs. 5(a) and 5(b). The results are presented in Figs. 5(c) and 5(d). When the data are shown that way, the changes from one sample to another can be acknowledged more easily. The first relaxation observed in the blend spectra corresponds to mainly PMMA and minorly PS chain relaxation. The second relaxation phenomenon is due to the relaxation of the droplets shape (τ_F). It can be noticed that this second relaxation is of the same order than the second relaxation in neat PS' relaxation spectra. However, due to its very low concentration, PS' contribution to the relaxations of blends is considered negligible. The third relaxation that is observed only in the case of BC2 [Fig. 5(d)] is due to Marangoni stresses (τ_β). As generally observed in the literature, Fig. 5(d) shows that this relaxation time decreases with the addition of BC [15,18]. This shows that BC2 is at least partially at the interface and a compatibilization mechanism should be observed.

The absence of these Marangoni stresses in the case of BC1 is probably due to the difference in molar mass as it is the only difference between BC1 and BC2. Knowing that Marangoni stresses relaxation is induced by movements of BC at the interface, BC1 should have a shorter Marangoni's relaxation: It has a smaller molar mass so it should be able to move faster. As such, the relaxation of the droplets and Marangoni's relaxation may be overlapped or close enough to be not distinguishable in Fig. 5(c).

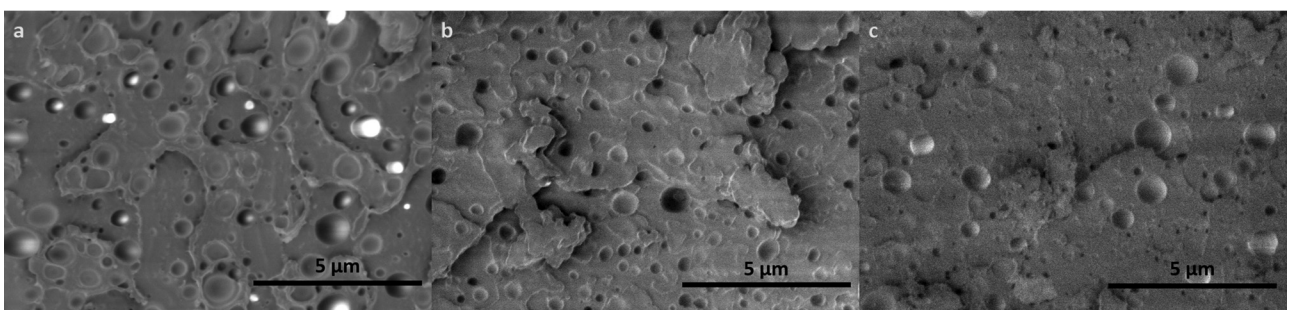

FIG. 3. Morphology of (a) pure PMMA/PS blend and blends with (b) 1% of BC1 and (c) 1% of BC2.

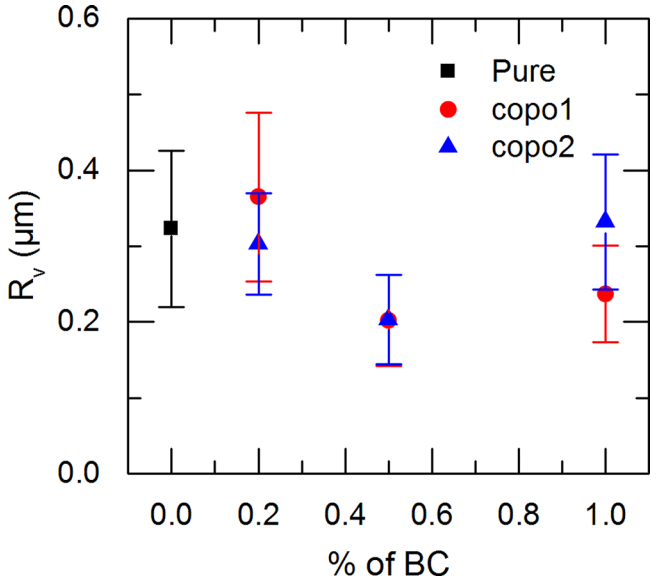

FIG. 4. Evolution of the volume average droplet radius with the addition of BC.

To verify this assumption, other rheological measurements were conducted at lower temperature: As already shown by Genoyer *et al.* [29], Marangoni's relaxation is influenced by temperature. By decreasing the temperature, the movements of BCs at the interface will be longer as the viscosity increases. As predicted, at 180 °C, the third relaxation corresponding to Marangoni stresses appears (see Fig. 6) for BC1. The relaxation time corresponding to relaxation of Marangoni stresses is not seen for 0.2% of BC1 as the amount of BC might be too low or the relaxation time too long to be observed. This confirms that BC1 is also at least partially at the interface, that the two relaxations were at similar times at 200 °C, and that Marangoni stresses are more influenced by temperature than the droplet shape relaxation. For the next results, the relaxation at 200 °C for BC1 blends is considered to be representative of the droplets shape relaxation.

By extracting the droplet shape relaxation time (τ_F) and using Eq. (5), the interfacial tension of each blend can be calculated. The interfacial tension between PMMA and PS can

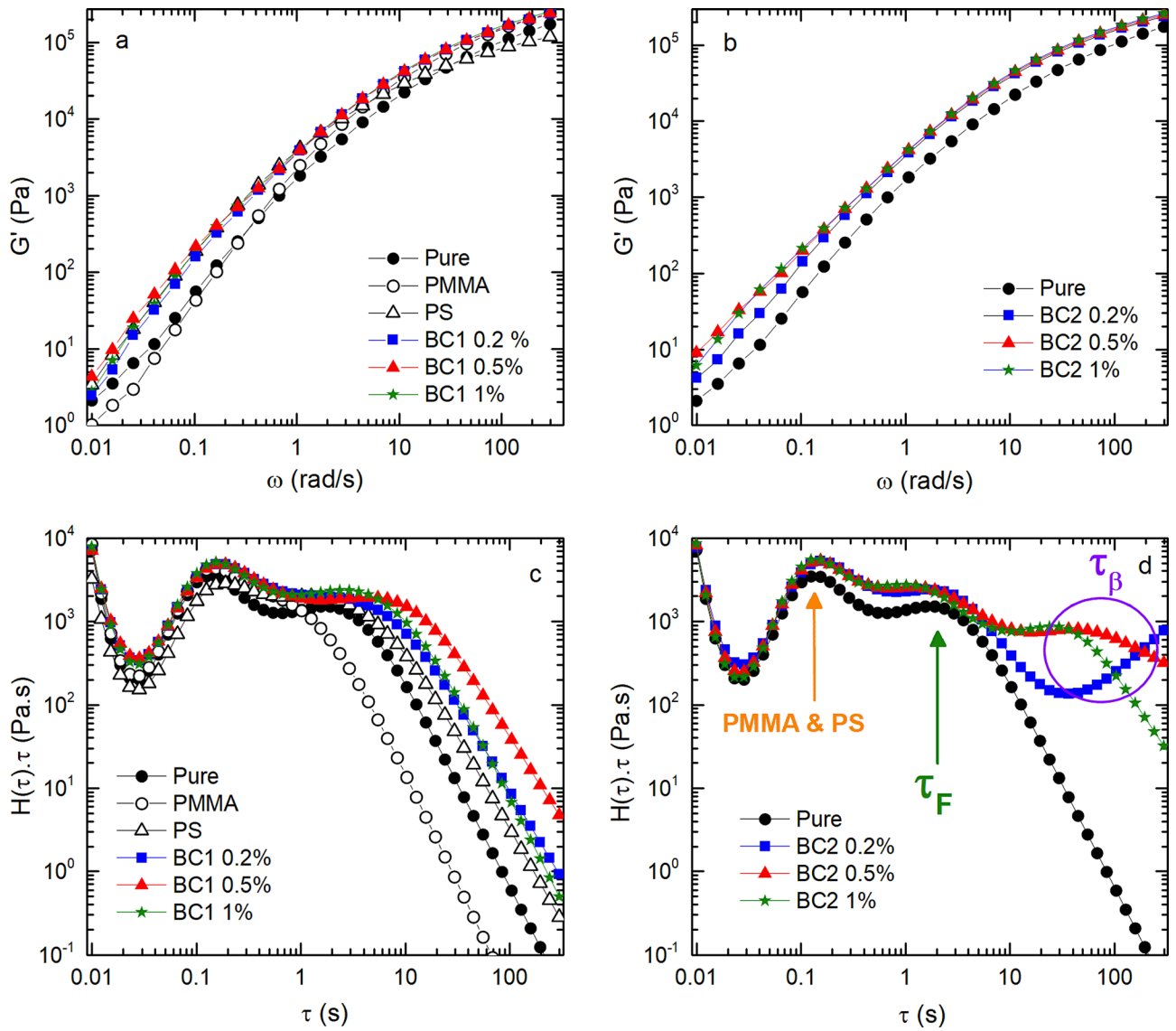

FIG. 5. SAOS results at 200 °C: Storage moduli of blends with (a) BC1, (b) BC2 and the relaxation spectra of blends with (a) BC1 and (b) BC2.

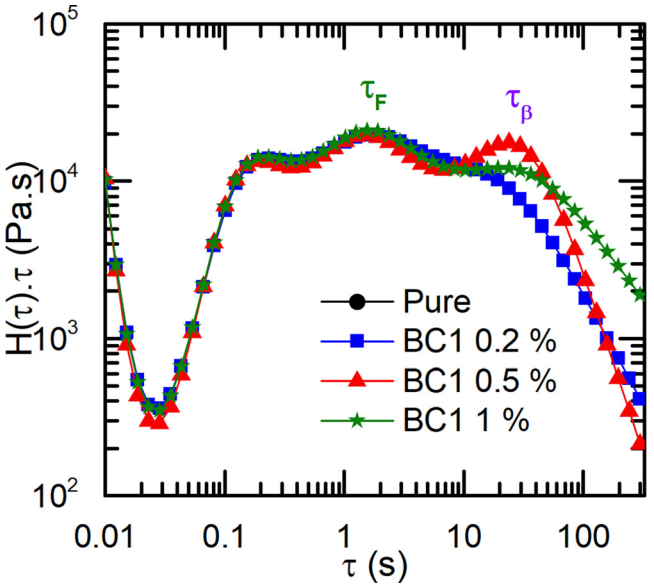

FIG. 6. Relaxation spectra of blends with addition of BC1 at 180 °C.

be found in the literature to be between 1 and 3 mN/m [8,15,29,31]. The values found here are of the same orders of magnitude, which decrease with the addition of BC1 but increase with the addition of BC2 (see Table III).

A decrease in interfacial tension and the presence of Marangoni stresses clearly attest the presence of BCs interface and that there should be a compatibilization effect. As generally Marangoni stresses are associated with coalescence suppression, coalescence tests were conducted to ensure the results reported here.

C. Coalescence

Coalescence tests were carried out following the shear history described in Part II. The results for BC1 are shown in Fig. 7. An evolution of the storage modulus at low frequencies can be witnessed. To understand better this evolution, three storage moduli predicted by the simplified Palierne model [28] were plotted in Fig. 8. P0.37 is the actual fit of the simplified Palierne model to experimental data for BC1 0.2% at strain = 0, with $R_v = 0.37\ \mu$m (determined previously by SEM). P0.037 and P3.7 curves are the model predictions with the parameters determined previously except R_v that is changed to 0.037 and 3.7 μm, respectively. The aim is to understand the evolution of the storage modulus when the droplets size changes. Figure 8 shows that the shoulder for which the droplets relaxation is responsible, indicated by arrows, shifts to lower frequencies when R_v increases and is more pronounced while doing so. This is the same type of evolution as observed in Fig. 7 during coalescence experiments. This increase in R_v is the evidence that coalescence occurred during the tests.

To analyze the coalescence phenomenon, the relaxation spectra for the different blends were inferred from the SAOS data reported in Fig. 7. In the case of BC1 (see Fig. 9), the evolution of the droplets' relaxation time (second relaxation) is very clear and shifts to greater values during the experiment. Indeed, the bigger the droplets, the more they will be deformed during shearing, therefore the longer the relaxation time of the shape after deformation. In the case of BC2, the results are slightly different because of Marangoni's relaxation: The relaxation of the droplets disappears starting at a strain of 100 for BC2 0.5% and 1%. This is most likely due to the fact that the shape and Marangoni's relaxation times are overlapping.

The evolution of the volume average radius was then calculated using τ_F extracted from the relaxation spectra (see Figs. 9 and 10) for all the blends except BC2 0.5% and 1%, where τ_F was used only until strain = 100. To do so, Eq. (5) was used and the interfacial tension was taken as calculated previously for strain = 0 and its variation during coalescence test was assumed negligible. Because of the disappearance of τ_F for 0.5% and 1% of BC2, τ_β was used to determine R_v. First, Eqs. (6)–(9) were used to determine the interface parameter β_{20} at strain = 0 necessary for further calculation. β_{20} was shown to increase when the amount of compatibilizer increases (see Table IV) which was already shown in other works [14,18]. It is also shown in Table IV that adjusting the β_{20} parameter with the value of ${\tau_\beta}^E$ and then calculating the theoretical ${\tau_F}^T$ leads to a very good agreement with the ${\tau_F}^E$ extracted directly from the relaxation spectra. This very good agreement confirms the fact that the second relaxation corresponds to the droplet relaxation time (τ_F) and the third to Marangoni's relaxation (τ_β).

For more clarity on the evolution of Marangoni's relaxation during the test, the values of τ_β were extracted from the relaxation spectra and plotted in Fig. 11. Two regimes can be observed: A decrease until a stationary value. As τ_β decreases with time, the calculated R_v decreases because Palierne's model predicts that τ_β varies with R_v [see Eqs. (6)–(9)]. It is the first time that such results were found: Our results differ completely from the observations of Van Hemelrijck *et al.* [17] who found that τ_β increased during coalescence tests such as predicted in Palierne's model because the larger the droplets, the longer the distance required for the BC to relax back to a uniform concentration. Because of the unusual evolution of τ_β, it was preferred to fit Palierne's model [28] on the storage modulus directly for blends with 0.5% and 1% of BC2 and for strain = 100, 250, and 1000. This way the exact value of τ_F is not required. The

TABLE III. α the interfacial tension calculated using R_v from SEM observation and τ_F from the relaxation spectra of each blend. Errors originate directly from the error on the R_v determined by SEM.

Blend		BC1			BC2		
%BC	Pure	0.2	0.5	1	0.2	0.5	1
α (mN/m)	4.3 ± 1.4	2.2 ± 0.7	0.6 ± 0.2	1.0 ± 0.3	3.0 ± 0.7	3.6 ± 0.9	6.9 ± 1.8

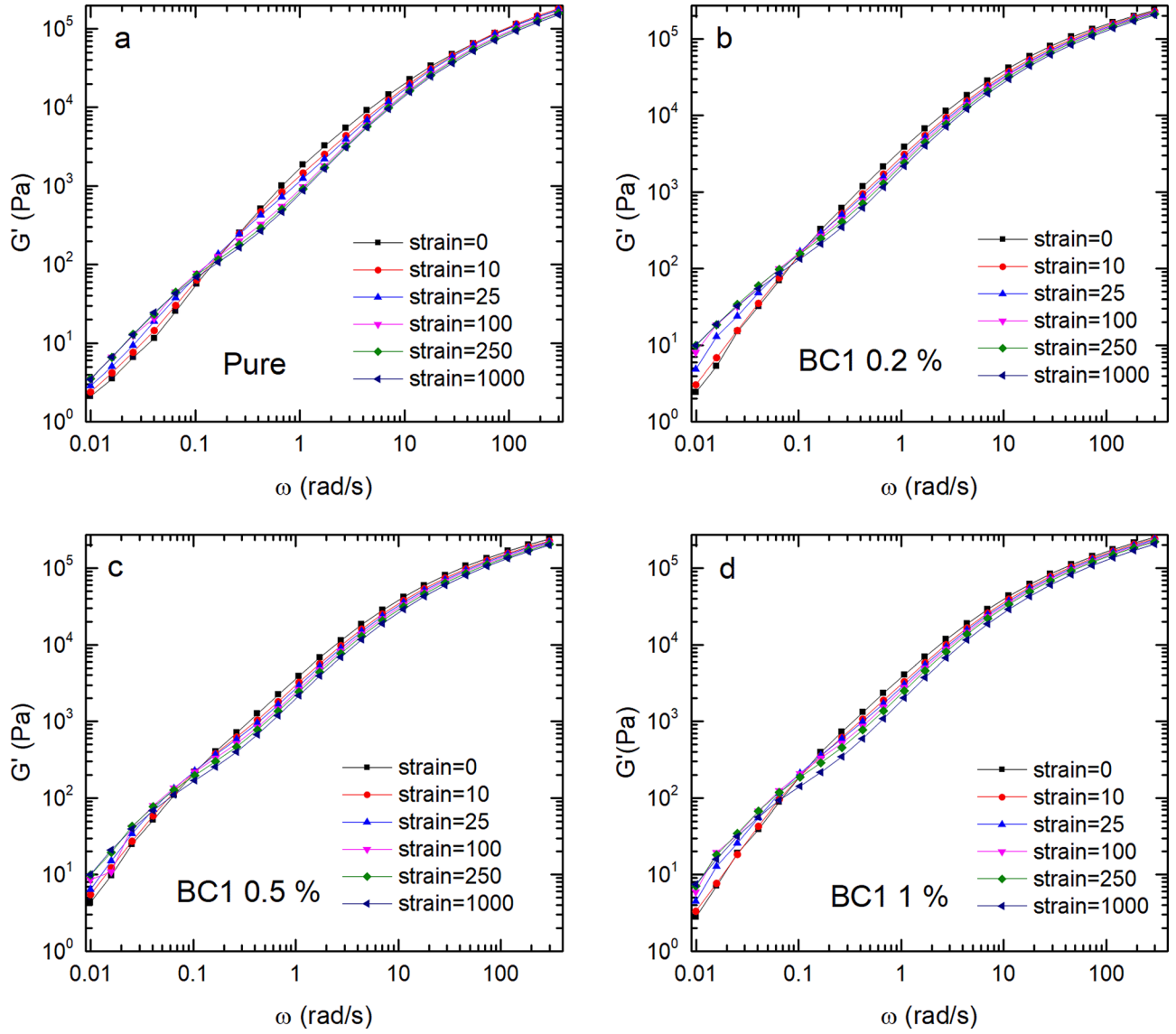

FIG. 7. SAOS measurements from the coalescence tests of blends containing BC1.

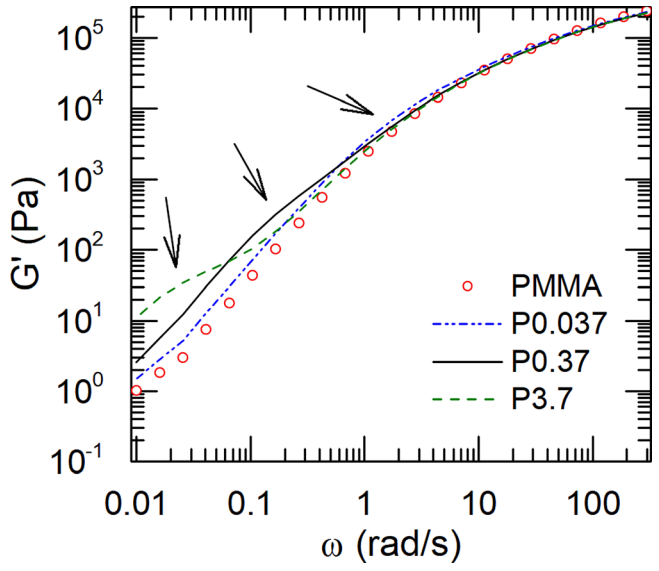

FIG. 8. Evolution of storage modulus predicted by Palierne's model when R_v varies.

results show a slight increase in R_v and are reported in Fig. 14 along with the results extracted from the relaxation spectra.

One explanation for τ_β's evolution previously reported in Fig. 11 could be that 7 min of mixing was not enough for the BC to migrate entirely to the interface, so the decrease in τ_β would be due to an increase in BC concentration at the interface rather than coalescence. This would explain the evolution of τ_β: It would decrease over time when BCs are still migrating to the interface, and it would stay constant when all the BCs are at the interface (starting around strain = 100). To verify this assumption, the blend with 0.5% of BC2 was prepared again using a longer mixing time (20 min).

The same experiments were conducted on this blend, named here BC2 0.5%–20 min. Figure 12 shows the evolution of the relaxation spectra of the new blend at strain = 0 and compares it to the previous blends with BC2. In Fig. 12(b), the droplets' relaxation seems slightly shorter for BC2 0.5%–20 min, which is due to a smaller droplets' size

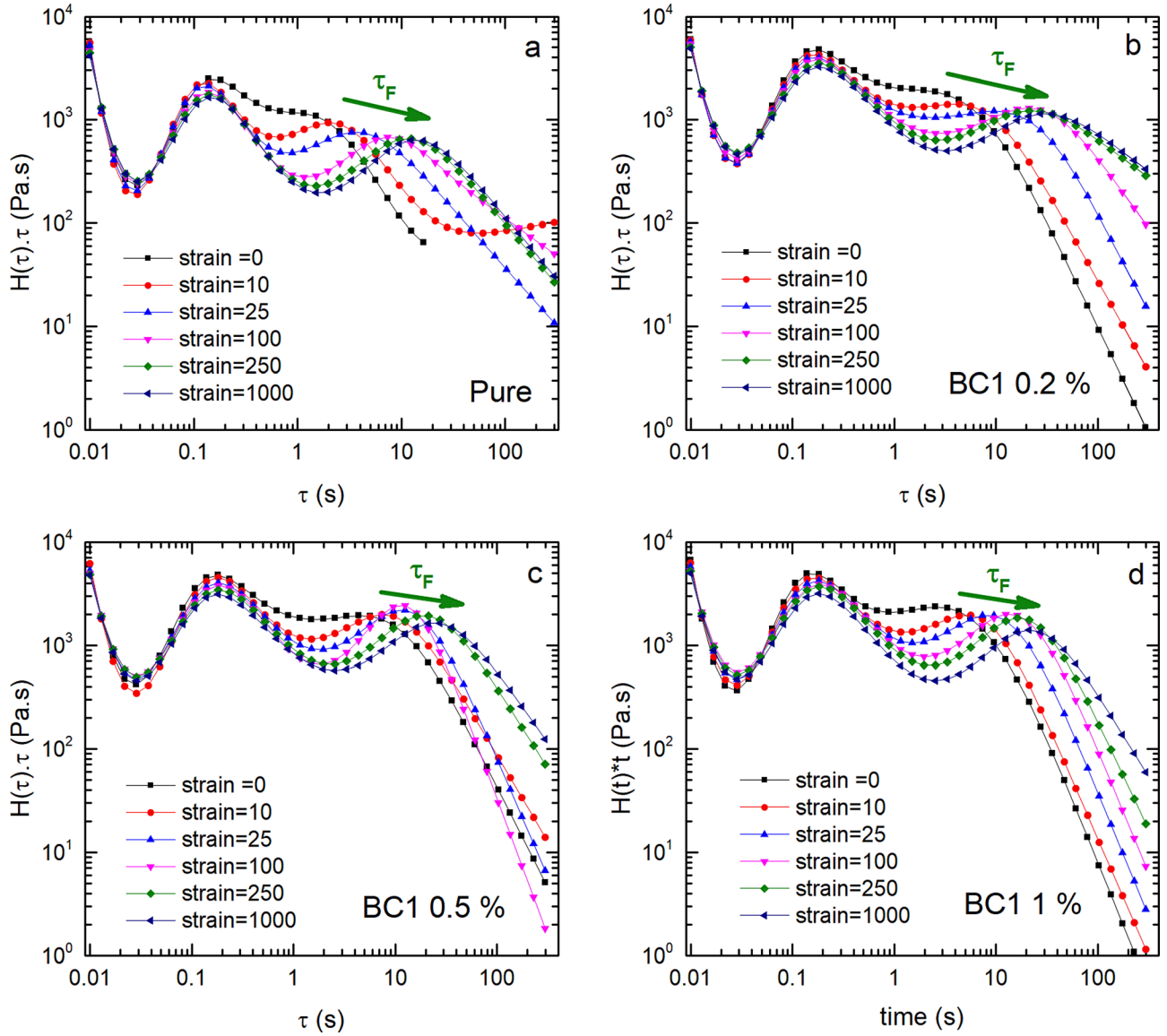

FIG. 9. Relaxation spectra of the blends containing BC1 during coalescence test.

as confirmed by SEM observations which showed a volume average radius of 0.152 μm. Moreover, using this R_v and Palierne's model, the interfacial tension was shown to be 3.2 mN/m, which is smaller than when the blend was mixed for 7 min. It also shows that Marangoni's relaxation is shorter when the blend is mixed for 20 min (BC2 0.5%–20 min) than for 7 min (BC2 0.5%) and the relaxation peak is sharper. The evolution of τ_β during coalescence experiments is reported in Fig. 13. It can be clearly seen that the relaxation times are smaller for BC2 0.5%–20 min during the whole experiment. However, the same previously observed evolution was found: A decrease until strain = 100. This evolution is clearly less pronounced than for both BC2 0.5% and 1%: The magnitude of the decrease in τ_β is 44% whereas previously it was 62%. It seems to us that this indicates that initially there is more BC at the interface and therefore less important migration. These results explain the evolution of morphology observed previously: There are no refinements as compatibilizer is added because there is not enough BC at the interface initially.

The evolution of R_v can be seen in Fig. 14. BC of 0.2% does not influence the coalescence process as no difference with the pure blend is observed. At higher BC content, 0.5% and 1%, a decrease in coalescence is observed. In addition, it seems that BC2 has a stronger influence compared to BC1 and therefore is more efficient. Surprisingly, it also seems that 0.5% is slightly better than 1%.

All the samples after coalescence were observed with SEM to confirm results obtained by rheology. Figure 15 shows the volume average radii after coalescence found with both rheology and SEM. Relatively good agreements were found for blends with 0.5% and 1% of BC. However, blends with 0.2% of BC show a huge disagreement between rheology results and SEM observations. We do not have an explanation for that important difference. However, those results confirm that BC2 is slightly more efficient than BC1.

To understand why BC2 is more efficient, the theoretical surface coverage was calculated using Eq. (11) extracted from the work of Lyu *et al.* [13]. Here the BC is supposed to be at the interface only. The results reported in Table V

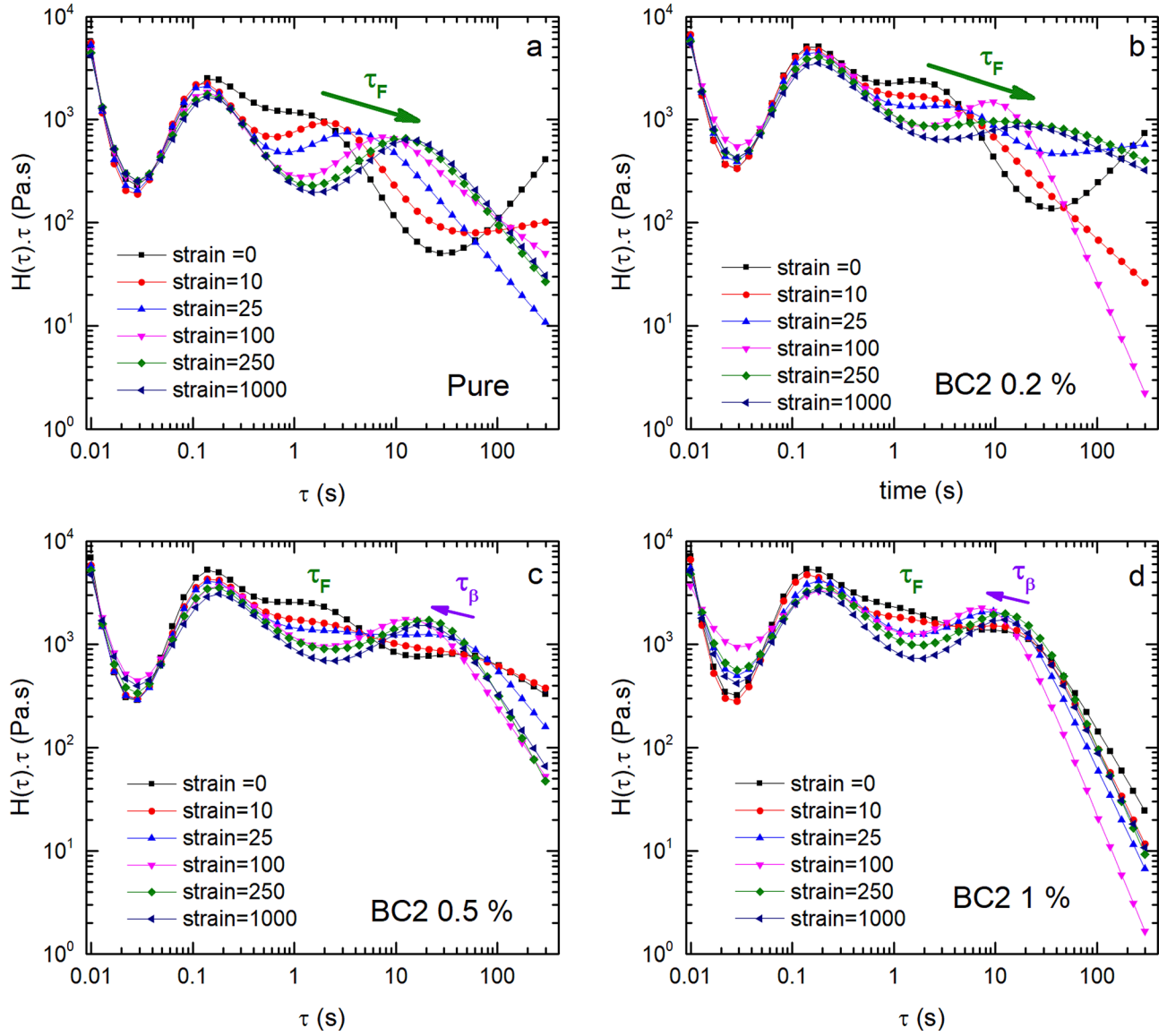

FIG. 10. Relaxation spectra of the blends containing BC2 during coalescence test.

show very low values compared to Adedeji *et al.* [24] who found values around 0.1–0.2 chain/nm^2. This is mainly because we use less BCs: They used 5–30% of BC whereas our highest concentration is 1%. According to those results, BC1 blends have a more important quantity of copolymer chains at the interface. This is not surprising as BC1 has a smaller molar mass so for a same mass there is more BC1 macromolecules than in the case of BC2. By multiplying the surface coverage by the area one chain of BC can cover at the interface, the percentage of covered interface can be recovered (see Table V). It can be noted that due to its bigger

TABLE IV. Experimental values of relaxations times $\tau_F{}^E$ and $\tau_\beta{}^E$, β_{20} the interface parameter calculated, and $\tau_F{}^T$ the theoretical relaxation time of the droplets calculated after determining β_{20}.

%BC2	β_{20} (mN/m)	$\tau_\beta{}^E$ (s)	$\tau_F{}^E$ (s)	$\tau_F{}^T$ (s)
0.5	0.11	53.4	1.52	1.51
1	0.43	22.5	1.30	1.27

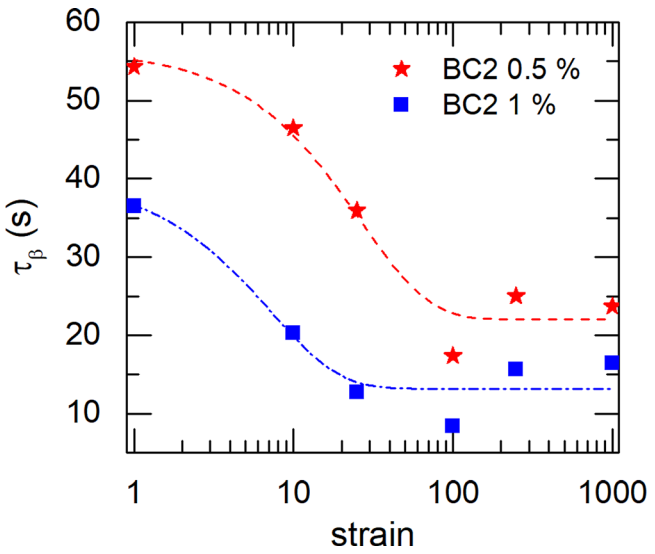

FIG. 11. Evolution of Marangoni's relaxation (τ_β) during coalescence tests, and dotted lines are exponential fits of the data.

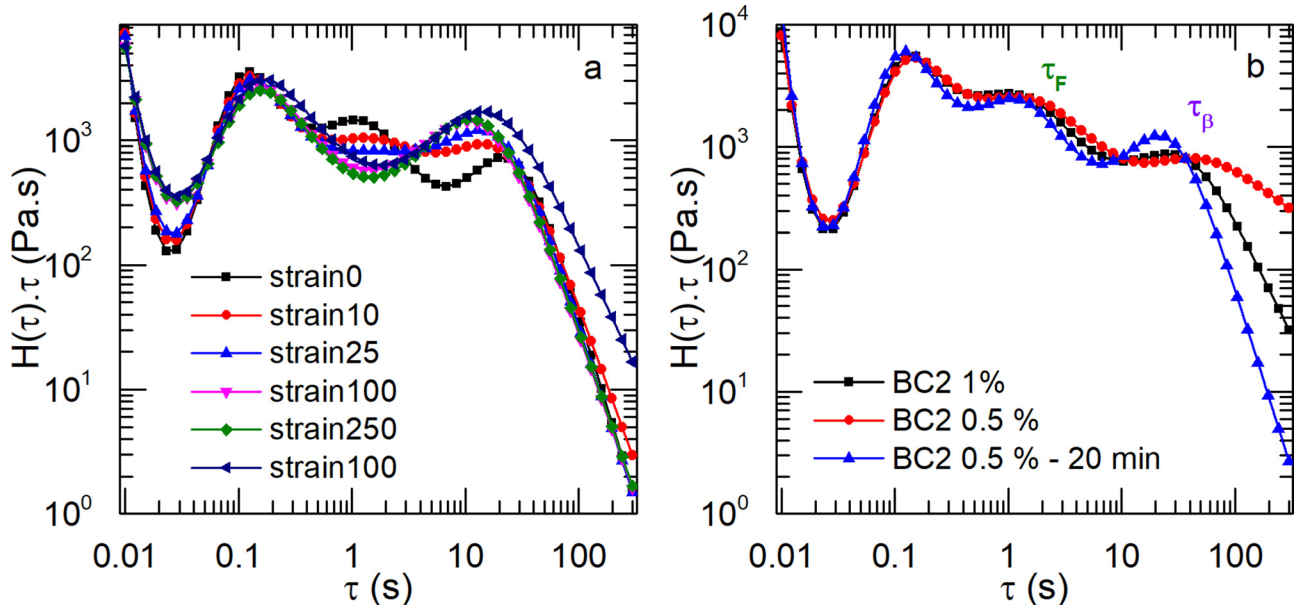

FIG. 12. (a) Evolution of BC2 0.5%–20 min during coalescence tests; (b) comparison of the relaxation spectra of blends containing 0.5% and 1% of BC2.

size, BC2 covers more interface than BC for a weight concentration of 1%. However, for 0.5% of BC, the percentage of covered interface is similar but BC2 is more efficient,

$$\sum = \frac{\Phi_{BC}}{\Phi_{PS}} \frac{R_v \rho_{BC} N_A}{6 M_{wBC}}. \tag{11}$$

Using Eq. (3) from Milner and Xi's work defining the minimum surface coverage needed to suppress coalescence and Eq. (9), the minimum percentage of BC needed can be found [32]. The results are 0.05% for BC1 and 0.16% for BC2. It shows that both BCs should suppress coalescence even with 0.2%. This would indicate again that BCs are not completely at the interface initially. The theory shows again that BC1 should be more efficient than BC2 as a smaller percentage should be required to suppress coalescence. However, both SEM and rheological results agree on the fact that BC2 is more efficient. As Milner and Xi based their equation on Marangoni stresses, it seems logical that BC1 should be more efficient as it can move more easily around the interface due to its small molecular mass. As such, the efficiency of BC2 may not be due to Marangoni stresses but to a better steric hindrance.

On this matter, Macosko *et al.* [33] assumed that coalescence inhibition arises from the steric repulsive forces from BCs at the surface of two approaching droplets. They estimated the minimum surface coverage for coalescence suppression to be as in Eq. (4) described previously.

This minimum surface coverage is reported in Table VI. Contrary to Milner and Xi's work, the concentration of BC1 added to the blend needs to be three times larger than the one of BC2 to be efficient. By comparing $\sum_c$ to $\sum$, the theoretical surface coverage of the droplets of each blend, it can

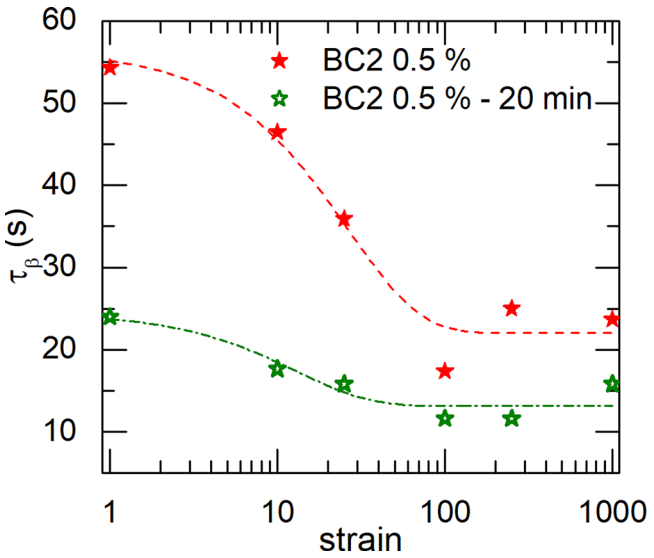

FIG. 13. Evolution of τ_β for blends with 0.5% of BC2 with 7 min (BC2 0.5%) and 20 min of mixing (BC2 0.5%–20 min). Dotted lines represent exponential fits of the data.

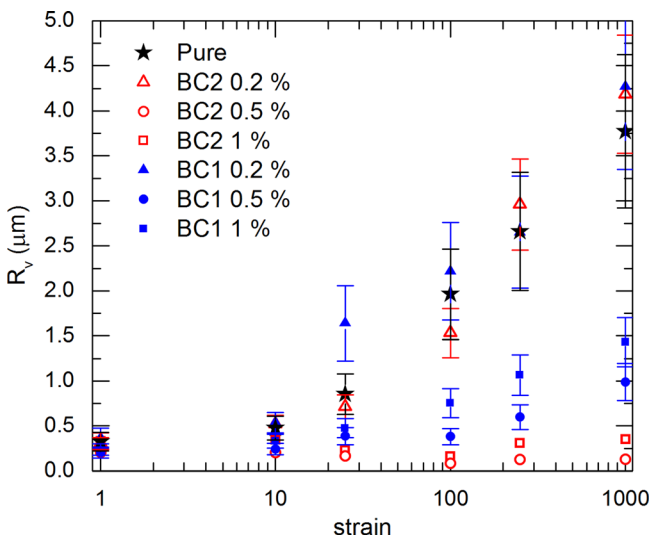

FIG. 14. Evolution of R_v during coalescence tests calculated using the Palierne model.

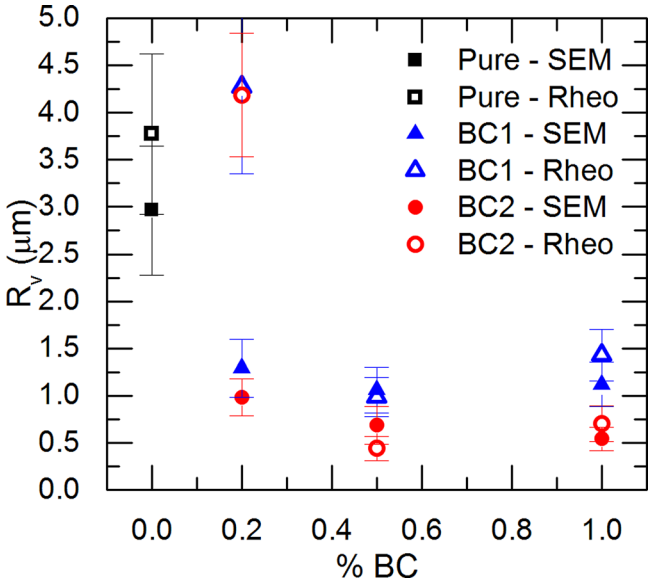

FIG. 15. Comparison of the R_v found by SAOS measurements and SEM after coalescence tests.

be noticed that both BC1 and BC2 should start to be efficient at 0.5%. BC2 is indeed efficient at 0.5% and 1%, but even if BC1 shows some improvement, it is still less efficient than BC2. Macosko *et al.* [33] had a similar result with a BC with a low molecular mass of 55 000 g/mol, suggesting that BC1 simply has a molecular mass too low to induce any steric hindrance.

This study leads us to think that steric hindrance and Marangoni stresses are both needed to be able to suppress coalescence as illustrated in Fig. 16. Indeed, Marangoni stresses are needed because if the BC is not distributed equally around the droplet, coalescence can happen easily [see Fig. 16(a)]. On the contrary, if there are Marangoni stresses but the BC is not big enough to induce steric hindrance, coalescence can be diminished but not completely suppressed as in the case of BC1 [see Fig. 16(c)]. Finally, Marangoni stress combined with a good steric hindrance can suppress coalescence as in the case of BC2 [Fig. 16(b)]. As such, an efficient coalescence suppression can be obtained at low concentration of BCs as the interface does not need to be saturated provided that the chosen compatibilizer induce enough steric hindrance.

IV. CONCLUSION

The aim of this work was to understand the compatibilization effect induced by two BCs with different molar masses.

TABLE V. Surface coverage.

	%BC	$\sum$ (chain/nm^2)	Covered interface (%)
BC1	0.2	0.0023	13
	0.5	0.0032	18
	1	0.0075	43
BC2	0.2	0.0006	11
	0.5	0.0009	19
	1	0.0030	60

TABLE VI. $\langle r_o^2 \rangle$ the square mean end-to end distance of the BC chains and $\sum_e$ the minimum surface coverage for coalescence suppression according to the steric hindrance theory.

	$\langle r_o^2 \rangle$ (nm)	$\sum_e$ (chain/nm^2)
BC1	65.8	0.0036
BC2	227.9	0.0010

The morphology was assessed by SEM and evidenced no refinement of the droplets's size contrary to what is expected. For further analysis, the rheological behavior was characterized.

The interfacial tension between the blend components for each blend was calculated using Palierne's model and relaxation spectra were inferred from SAOS results. A decrease in interfacial tension and the presence of Marangoni stresses were evidenced for blends containing BC1, indicating that at least part of BCs are at the interface and act as compatibilizers. To evidence these Marangoni stresses, lowering the temperature was necessary in the case of addition of BC with a low molar mass. Indeed, Marangoni's relaxation was too short and was not distinguishable from the droplet's shape relaxation. As lowering the temperature allowed to differentiate them, it proves that Marangoni stresses are much influenced by temperature, more than droplets' shape relaxation. In the case of blends with the addition of the BC with a higher molar mass, no decrease in interfacial tension was evidenced; however, Marangoni stresses were evidenced by relaxation spectra.

Knowing that Marangoni stresses helps to inhibit coalescence, shear induced coalescence tests were performed. Those tests resulted in the confirmation that the presence of BCs induces an inhibition of coalescence for both BCs. However, coalescence tests evidenced a decrease in Marangoni's relaxation during coalescence tests. This behavior was attributed to the fact that BCs were not fully at the interface after processing. Their migration to the interface during coalescence is an explanation for the decrease in τ_β and would also explain why there is no refinement of the morphology upon addition of copolymers: Initially, there is not enough BC at the interface. Finally, the BC with the higher molar mass was shown to be more efficient at inhibiting coalescence. However, if only Marangoni stresses were involved in the mechanism, the smaller BC should be more efficient as it can move faster around the interface. These results evidenced the importance of steric hindrance in the compatibilization mechanism. Higher molar mass of the BC results in more efficient repulsion between the droplets and thus decreased coalescence.

To conclude, the compatibilization mechanism in these systems was shown to be a combination of decrease in interfacial tension, Marangoni stresses, and steric hindrance.

ACKNOWLEDGMENTS

Financial support from the Natural Sciences and Engineering Research Council of Canada (NSERC) and Ecole de Technologie Supérieure (ETS) is gratefully acknowledged.

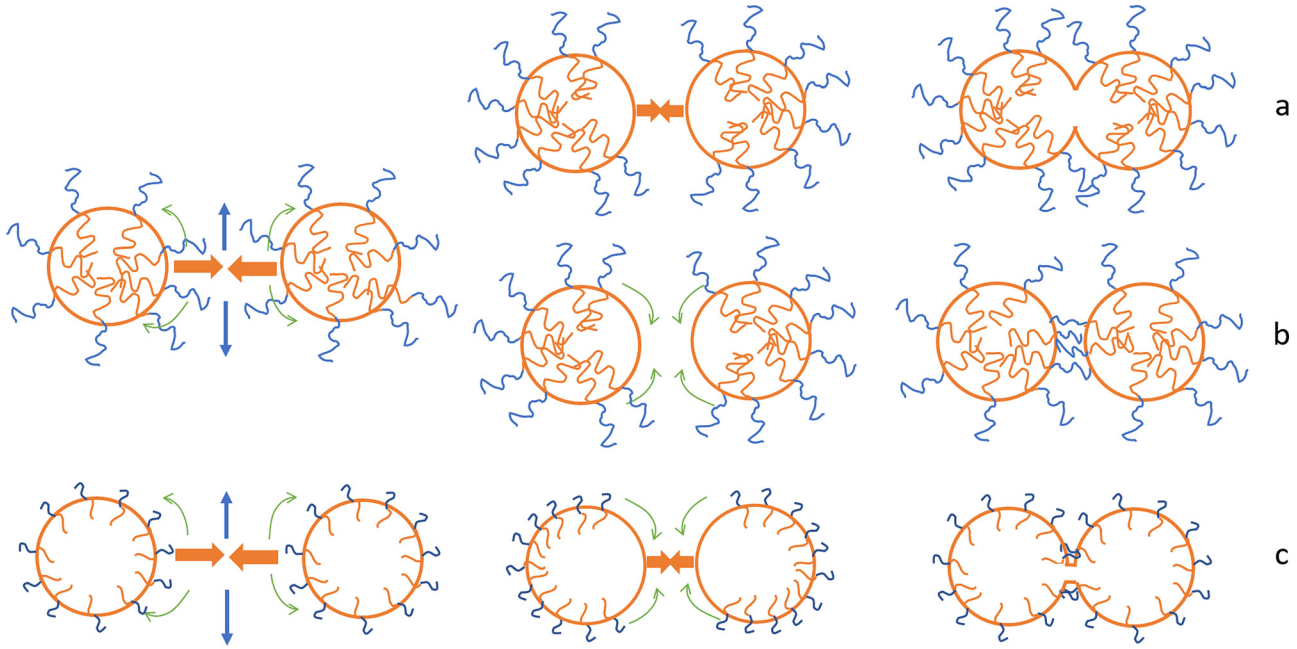

FIG. 16. Illustration of the compatibilization mechanism: (a) Steric hindrance without Marangoni stresses leads to coalescence, (b) Marangoni stresses combined with steric hindrance prevent coalescence, and (c) Marangoni stresses without steric hindrance does not suppress coalescence.

References

[1] Taylor, G. I., "The viscosity of a fluid containing small drops of another fluid," Proc. R. Soc. London., Ser. A **138**(834), 41–48 (1932).

[2] Grace, H. P., "Dispersion phenomena in high viscosity immiscible fluid systems and application of static mixers as dispersion devices in such systems," Chem. Eng. Commun. **14**(3–6), 225–277 (1982).

[3] Van Puyvelde, P. V., and P. Moldenaers, "Rheology and morphology development in immiscible polymer blends," Rheol. Rev. 101–145 (2005).

[4] Tucker, C. L., and P. Moldenaers, "Microstructural evolution in polymer blends," Annu. Rev. Fluid Mech. **34**, 177–210 (2002).

[5] DeLeo, C. L., and S. S. Velankar, "Morphology and rheology of compatibilized polymer blends: Diblock compatibilizers vs crosslinked reactive compatibilizers," J. Rheol. **52**(6), 1385–1404 (2008).

[6] Souza, A. M. C., and N. R. Demarquette, "Influence of coalescence and interfacial tension on the morphology of PP/HDPE compatibilized blends," Polymer **43**(14), 3959–3967 (2002).

[7] Macaubas, P. H., and N. Demarquette, "Morphologies and interfacial tensions of immiscible polypropylene/polystyrene blends modified with triblock copolymers," Polymer **42**(6), 2543–2554 (2001).

[8] Yee, M., P. S. Calvão, and N. R. Demarquette, "Rheological behavior of poly(methyl methacrylate)/polystyrene (PMMA/PS) blends with the addition of PMMA-ran-PS," Rheol. Acta **46**(5), 653–664 (2007).

[9] Sundararaj, U., and C. W. Macosko, "Drop breakup and coalescence in polymer blends : The effects of concentration and compatibilization," Macromolecules **28**(8), 2647–2657 (1995).

[10] Ramic, A. J., J. C. Stehlin, S. D. Hudson, A. M. Jamieson, and I. Manas-Zloczower, "Influence of block copolymer on droplet breakup and coalescence in model immiscible polymer blends," Macromolecules **33**(2), 371–374 (2000).

[11] Huitric, J., M. Moan, P. J. Carreau, and N. Dufaure, "Effect of reactive compatibilization on droplet coalescence in shear flow," J. Non-Newtonian Fluid Mech. **145**(2–3), 139–149 (2007).

[12] Vermant, J., G. Cioccolo, K. Golapan Nair, and P. Moldenaers, "Coalescence suppression in model immiscible polymer blends by nano-sized colloidal particles," Rheol. Acta **43**(5), 529–538 (2004).

[13] Lyu, S., T. D. Jones, F. S. Bates, and C. W. Macosko, "Role of block copolymers on suppression of droplet coalescence," Macromolecules **35**(20), 7845–7855 (2002).

[14] de Souza, A. M. C., P. S. Calvão, and N. R. Demarquette, "Linear viscoelastic behavior of compatibilized PMMA/PP blends," J. Appl. Polym. Sci. **129**(3), 1280–1289 (2013).

[15] Jacobs, U., M. Fahrländer, J. Winterhalter, and C. Friedrich, "Analysis of Palierne's emulsion model in the case of viscoelastic interfacial properties," J. Rheol. **43**(6), 1495–1509 (1999).

[16] Van Hemelrjick, E., P. Van Puyvelde, S. Velankar, C. W. Macosko, and P. Moldenaers, "Interfacial elasticity and coalescence suppression in compatibilized polymer blends," J. Rheol. **48**(1), 143–158 (2003).

[17] Van Hemelrijck, E., P. Van Puyvelde, C. W. Macosko, and P. Moldenaers, "The effect of block copolymer architecture on the coalescence and interfacial elasticity in compatibilized polymer blends," J. Rheol. **49**(3), 783–798 (2005).

[18] Riemann, R., H. Cantow, and C. Friedrich, "Interpretation of a new interface-governed relaxation process in compatibilized polymer blends," Macromolecules **30**(18), 5476–5484 (1997).

[19] Friedrich, C., and Y. Y. Antonov, "Interfacial relaxation in polymer blends and gibbs elasticity," Macromolecules **40**(4), 1283–1289 (2007).

[20] Fortelný, I., "An analysis of the origin of coalescence suppression in compatibilized polymer blends," Eur. Polym. J. **40**(9), 2161–2166 (2004).

[21] Van Puyvelde, P., S. Velankar, J. Mewis, P. Moldenaers, and K. U. Leuven, "Effect of marangoni stresses on the deformation and coalescence in compatibilized immiscible polymer blends," Polym. Eng. Sci. Sci. **42**(10), 1956–1964 (2002).

[22] Calvão, P. S., M. Yee, and N. R. Demarquette, "Effect of composition on the linear viscoelastic behavior and morphology of PMMA/PS and PMMA/PP blends," Polymer **46**(8), 2610–2620 (2005).

[23] Jeon, H. K., and C. W. Macosko, "Visualization of block copolymer distribution on a sheared drop," Polymer **44**(18), 5381–5386 (2003).

[24] Adedeji, A., S. Lyu, and C. W. Macosko, "Block copolymers in homopolymer blends: Interface vs micelles," Macromolecules **34**(25), 8663–8668 (2001).

[25] Graebling, D., R. Muller, and J. F. Palierne, "Linear viscoelastic behavior of some incompatible polymer blends in the melt. Interpretation of data with a model of emulsion of viscoelastic liquids," Macromolecules **26**(2), 320–329 (1993).

[26] Honerkamp, J., and J. Weese, "A nonlinear regularization method for the calculation of relaxation spectra," Rheol. Acta **32**(1), 65–73 (1993).

[27] Palierne, J. F., "Linear rheology of viscoelastic emulsions with interfacial tension," Rheol. Acta **29**(3), 204–214 (1990).

[28] Bousmina, M., P. Bataille, S. Sapieha, and H. P. Schreiber, "Comparing the effect of corona treatment and block copolymer addition on rheological properties of polystyrene/polyethylene blends," J. Rheol. **39**(3), 499–517 (1995).

[29] Genoyer, J., M. Yee, J. Soulestin, and N. Demarquette, "Compatibilization mechanism induced by organoclay in PMMA/PS blends," J. Rheol. **61**(4), 613–626 (2017).

[30] Vinckier, I., P. Moldenaers, A. M. Terracciano, and N. Grizzuti, "Droplet size evolution during coalescence in semiconcentrated model blends," AIChE J. **44**(4), 951–958 (1998).

[31] Yee, M., A. M. C. Souza, T. S. Valera, and N. R. Demarquette, "Stress relaxation behavior of PMMA/PS polymer blends," Rheol. Acta **48**(5), 527–541 (2009).

[32] Milner, S. T., and H. Xi, "How copolymers promote mixing of immiscible homopolymers," J. Rheol. **40**(4), 663–683 (1996).

[33] Macosko, C. W., P. Guégan, A. K. Khandpur, A. Nakayama, P. Marechal, and T. Inoue, "Compatibilizers for melt blending: Premade block copolymers," Macromolecules **29**(96), 5590–5598 (1996).